Inorg. Chem. **2006**, *45*, 9569–9579

Electrochemistry of Aluminum Phthalocyanine: Solvent and Anion Effects on UV–Visible Spectra and Reduction Mechanisms

Zhongping Ou,[†,‡] Jing Shen,[‡] and Karl M. Kadish*[,‡]

Department of Applied Chemistry, Jiangsu University, Zhenjiang, Jiangsu 212013, China, and Department of Chemistry, University of Houston, Houston, Texas 77204-5003

Received June 14, 2006

The electrochemistry and UV–vis spectral properties of neutral and electroreduced Al(III) phthalocyanine, (Pc)AlCl, were characterized in four different nonaqueous solvents (THF, DMSO, DMF, and pyridine) containing tetra-*n*-butylammonium perchlorate, as well as in THF containing 0.4 M TBAP and the more strongly coordinating Cl^-, F^-, OH^-, or CN^- anions added to solution in the form of a tetra-*n*-butylammonium salt. The initial phthalocyanine added to solution is represented as (Pc)AlCl, but the actual electroactive form of the compound varied as a function of both the solvent and type or number of bound anionic axial ligands. An uncharged (Pc)AlCl(THF) or (Pc)Al-(CN)(THF) complex is present in THF solutions containing 0.4 M TBAP and excess Cl^- or CN^-, while transient μ-oxo dimers are spectroscopically observed upon addition of OH^- or F^- to (Pc)AlCl(THF) in THF followed by the ultimate formation of stable six-coordinate anionic species represented as $[(Pc)Al(OH)_2]^-$ or $[(Pc)AlF_2]^-$. Each phthalocyanine undergoes three reversible one-electron additions at the conjugated Pc macrocycle within the negative potential limit of the solvent, and the UV–vis spectral changes obtained during the first two reductions were recorded in a thin-layer cell to evaluate the prevailing electron-transfer mechanisms.

Introduction

Aluminum porphyrins and phthalocyanines are of interest because of their possible applications in the area of new functional materials.[1−4] The Al(III) form of these compounds has a high binding affinity with the fluoride ion,[5−14] and a highly selective optical fluoride ion sensor based on aluminum(III) octaethylporphyrin has been described in a recent communication.[9] The development of new applications for the use of aluminum phthalocyanines in material science requires, in many cases, a detailed knowledge of the compounds' electrochemical reactivity, but only a few studies of aluminum phthalocyanine electrochemistry in nonaqueous media have been reported,[15−20] none of which presents a detailed mechanistic study of the electron-transfer reactions. In addition, the published reports are somewhat contradictory about the number of redox processes which can be observed. For example, cyclic voltammetric studies of (Pc)AlCl at a Pt electrode in dimethylacetamide (DMA) showed three one-

* To whom correspondence should be addressed. E-mail: kkadish@uh.edu.
† Jiangsu University.
‡ University of Houston.

(1) *The Porphyrin Handbook*; Kadish, K. M., Smith, K. M., Guilard, R., Eds.; Academic Press: Amsterdam, 1999; Vols. 1−10; 2003, Vols. 11−20.
(2) Buehlmann, P.; Pretsch, E.; Bakker, E. *Chem. Rev.* **1998**, *98*, 1593−1687.
(3) Bakker, E.; Meyerhoff, M. E. In *Bioelectrochemistry*; Bard, A. J., Stratmann, M., Wilson, G. S., Eds.; Wiley: New York, 2002; Vol. 9, pp 279−307.
(4) Gorski, L.; Malinowska, E.; Parzuchowski, P.; Zhang, W.; Meyerhoff, M. E. *Electroanalysis* **2003**, *15*, 1229−1235.
(5) Kotrly, S.; Sucha, L. *Handbook of Chemical Equilibria in Analytical Chemistry*; Wiley and Sons: New York, 1985.
(6) Martell, A. E.; Smith, R. M. *Critical Stability Constants*; Plenum Press: New York, 1974.
(7) Steinle, E. D.; Schaller, U.; Meyerhoff, M. E. *Anal. Sci.* **1998**, *14*, 79−84.
(8) Malinowska, E.; Gorski, L.; Meyerhoff, M. E. *Anal. Chim. Acta* **2002**, *468*, 133−141.
(9) Badr, I. H. A.; Meyerhoff, M. E. *J. Am. Chem. Soc.* **2005**, *127*, 5318−5319.
(10) Shapovalov, V. L.; Rokiskaya, T. I.; Kotova, E. A.; Krokhin, O. V.; Antonenko, Y. N. *Photochem. Photobiol.* **2001**, *74*, 1−7.
(11) Rokiskaya, T. I.; Block, M. A.; Antonento, Y. N.; Kotova, E. A.; Pohl, P. A. N. *Biophys. J.* **2000**, *78*, 2572−2580.
(12) Rosenthal, I.; Shafirovich, V. Y.; Geacintov, N. E.; Ben-Hur, E.; Horowitz, B. *Photochem. Photobiol.* **1994**, *60*, 215−220.
(13) Ben-Hur, E.; Dubbelman, T. M.; Van Steveninck, J. *Photochem. Photobiol.* **1991**, *54*, 703−707.
(14) Badr, I. H. A.; Meyerhoff, M. E. *Anal. Chem.* **2005**, *77*, 6719−6728.
(15) Giraudeau, A.; Fan, F. F.; Bard, A. *J. Am. Chem. Soc.* **1980**, *102*, 5137−5142.
(16) Lexa, D.; Reix, M. *J. Chim. Phys.* **1974**, *71*, 511−513.
(17) Homborg, H.; Murray, K. S. *Z. Anorg. Allg. Chem.* **1984**, *517*, 149−160.
(18) Deng, X.; Porter, W. W., III; Vaid, T. P. *Polyhedron* **2005**, *24*, 3004−3011.
(19) Cissell, J. A.; Vaid, T. P.; Rheingold, A. L. *Inorg. Chem.* **2006**, *45*, 2367−2369.
(20) Lever, A. B. P.; Minor, P. C. *Inorg. Chem.* **1981**, *20*, 4015−4017.

10.1021/ic061072f CCC: $33.50
Published on Web 09/30/2006

electron reductions within the solvent potential limit,[15] but polarograms of the same compound at a dropping mercury electrode in *N*,*N*-dimethylformamide (DMF) indicated four reductions over the same potential range from 0.0 to −2.20 V vs SCE.[21] A recent electrochemical study of (Pc)AlCl in terahydrofuran (THF) showed two reductions,[19] while earlier electrochemical studies of the same compound in DMF[17] reported only a single one-electron reduction process.

The apparent variability in the number of observed redox reactions may be, in part, a result of the low solubility of Al(III) phthalocyanines, a difference between the different studies in the negative solvent potential range investigated, or the high tendency of these compounds to form μ-oxo dimers in the presence of trace water or hydroxide.[22] However, to our knowledge, there is only one brief report in the literature on the electrochemistry of a genuine Al(III) Pc μ-oxo dimer, $[(Pc)AlF]_2O$.[17] A summary of Al(III) phthalocyanine electrochemistry is given in a recent review by L'Her and Pondaven,[23] but it is not clear from the overall data how the electrochemistry is affected by changes in the solvent or by the addition of coordinating anions to solution. Therefore, to better understand the redox reactivity of aluminum phthalocyanine in different oxidation states, we have reinvestigated the electrochemistry and UV−vis spectral properties of neutral and electroreduced (Pc)AlCl in four different nonaqueous solvents (THF, DMSO, DMF, and pyridine) containing tetra-*n*-butylammonium perchlorate (TBAP), as well as in THF containing the more strongly coordinating Cl^-, F^-, OH^-, or CN^- anions in addition to 0.4 M TBAP. One goal of our study was to determine the nature of the electroactive species in solution, while another was to elucidate the solvent and anion effects on the number of observed reduction processes and their redox potentials. We also wished to provide the first definitive electroreduction mechanism for aluminum phthalocyanine in nonaqueous media and, at the same time, characterize the UV−vis spectra of the electroreduced species under different solution conditions.

Experimental Section

Instrumentation. Cyclic voltammetry was carried out with an EG & G model 173 potentiostat. A three-electrode system was used, and it consisted of a glassy carbon or platinum disk working electrode, a platinum wire counter electrode, and a saturated calomel reference electrode (SCE). The SCE electrode was separated from the bulk of the solution by a fritted-glass bridge of low porosity which contained the solvent/supporting electrolyte mixture. Ferrocene was added to the solution as an internal reference to check the potentials. UV−vis spectroelectrochemical experiments were performed with an optically transparent platinum thin-layer electrode.[24] Potentials were applied with an EG & G model 173 potentiostat. Time-resolved UV−vis spectra were recorded with a Hewlett-Packard model 8453 diode array rapid-scanning spectrophotometer.

(21) Clack, D. W.; Hush, N. S.; Woolsey, I. S. *Inorg. Chim. Acta* **1976**, *19*, 129−132.
(22) Linsky, J. P.; Paul, T. R.; Nohr, R. S.; Kenney, M. E. *Inorg. Chem.* **1980**, *19*, 3131−3135.
(23) L'Her, M.; Pondaven, A. In *The Porphyrin Handbook*; Kadish, K. M., Smith, K. M., Guilard, R., Eds.; Academic Press: Amsterdam, 2003; Vol. 16, Chapter 104, pp 117−169.
(24) Lin, X. Q.; Kadish, K. M. *Anal. Chem.* **1985**, *57*, 1489−1501.

Table 1. UV−Vis Spectral Data (λ_{max}, nm, $\epsilon \times 10^{-4}$) of Neutral (Pc)AlCl and Its Reduced Forms in Different Solvents Containing 0.1 M TBAP

	solvent	DN[a]	B band	Q band		
Pc(2−)	THF[b]	20	347 (2.4)	609 (1.6)	642 (1.4)	**675** (10.2)
	DMF	26.6	357 (5.0)	610 (2.5)	647 (2.3)	**677** (15.4)
	DMSO	29.8	358 (5.1)	613 (2.6)	651 (2.2)	**681** (16.8)
	py	33.1	364 (5.7)	614 (3.0)	651 (2.5)	**681** (18.5)
Pc(3−)	THF[b]		331 (4.1)	582 (4.0)	622 (3.5)	985 (0.7)
	DMF		332 (2.9)	580 (2.8)	621 (2.4)	969 (0.9)
	DMF[c]		329	575	618	974
	py		352 (4.1)	589 (6.6)	620 (4.3)	991 (1.0)
Pc(4−)	THF[b]		325 (3.6)	521 (3.4)		
	DMF		335 (2.4)	517 (3.7)		
	DMF[c]		327	518		
	py		320 (3.1)	524 (4.8)		

[a] Gutmann donor number taken from ref 26. [b] 0.4 M TBAP. [c] Ref 33.

Chemicals and Reagents. Tetrahydrofuran (THF, 99.9%), *N*,*N*-dimethylformamide (DMF, >99.9%), dimethyl sulfoxide (DMSO, ≥99.9%), pyridine (py, >99.9%), tetra-*n*-butylammonium chloride (TBACl), tetra-*n*-butylammonium fluoride trihydrate (TBAF·$3H_2O$), tetra-*n*-butylammonium cyanide (TBACN), aluminum phthalocyanine chloride ((Pc)AlCl), and aluminum phthalocyanine hydroxide ((Pc)Al(OH)) were obtained from Sigma-Aldrich Chemical Co. and used as received. Tetra-*n*-butylammonium hydroxide (TBAOH, 1.0 M solution in methanol) was purchased from Adrich Chemical Co., Inc., and was used as received. Tetra-*n*-butylammonium perchlorate (TBAP) was purchased from Fluka Chemical Co. and was twice recrystallized from absolute ethanol and dried in a vacuum oven at 40 °C for a week prior to use.

Results and Discussion

Effect of Solvent on UV−Vis Spectra of a Neutral Compound. The UV−vis spectrum of (Pc)AlCl was measured in THF, DMF, DMSO, and py prior to the electrochemical experiments being carried out, and the spectral data are summarized in Table 1 and Figure 1. In each solvent, the unreduced compound, represented as Pc(2−), is characterized by an intense Q band at 675−681 nm (shown in bold print in Table 1) and two additional bands in the visible region of the spectrum, located between 609 and 651 nm. There is also a broad B band at 347−364 nm, and these spectra are those of a "normal" monomeric phthalocyanine [Pc(2−)] having a +2 or +3 central metal ion.[25]

As seen in Table 1, the B and Q bands of (Pc)AlCl red shift and increase in molar absorptivity upon changing from the low-donor solvent THF to the high-donor solvent pyridine. The shift of the Q band position from 675 nm in THF to 681 nm in DMSO or py is consistent with solvent (S) binding to the Al(III) ion, giving either (Pc)AlCl(S) or $(Pc)Al(S)_x^+Cl^-$, where $x = 1$ or 2. Electrochemical experiments described on the following pages indicate that Cl^- remains associated to (Pc)AlCl in all four electrochemical solvents used, and this suggests that (Pc)AlCl(S) is the electroactive species with the prevailing solvent-binding reaction of the neutral phthalocyanine occurring as shown in eq 1.

$$(Pc^{2-})AlCl + S \rightleftharpoons (Pc^{2-})AlCl(S) \quad (1)$$

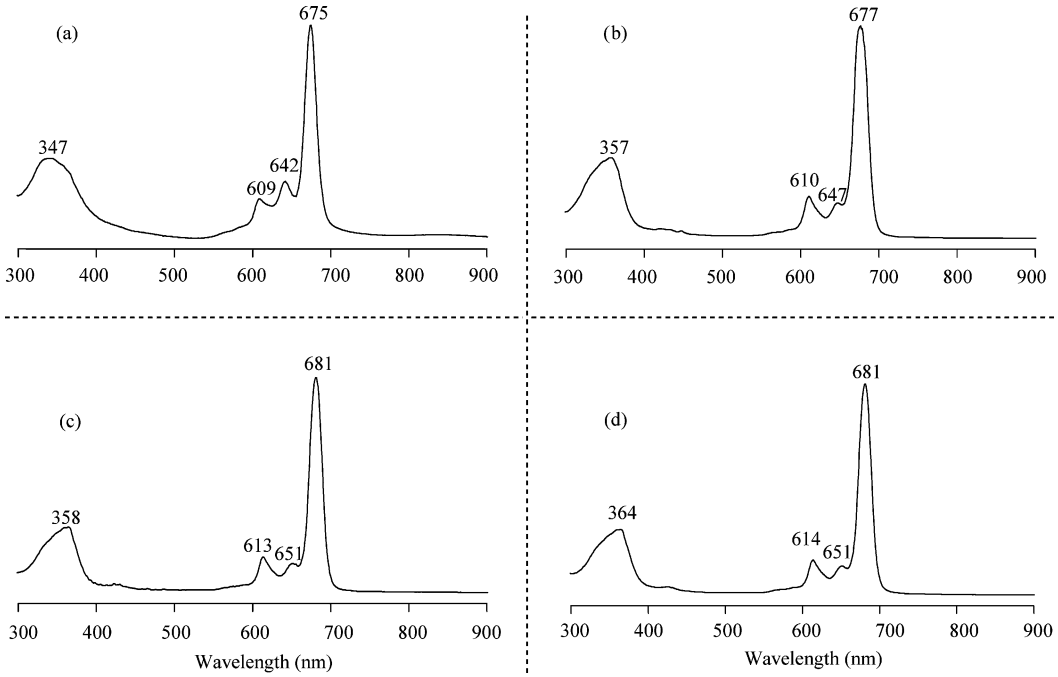

Figure 1. UV−vis spectra of (Pc)AlCl in the investigated solvents: (a) THF, (b) DMF, (c) DMSO, and (d) pyridine.

The relative binding strength of solvents used for electrochemical measurements can be qualitatively described by the Gutmann donor number (DN) which ranges from 0.00 for 1,2-dichloroethane to 38.8 for hexamethylphosphoric triamide.[26] The DN for solvents used in the present work follows the order: THF (20) < DMF (26.6) < DMSO (29.8) < pyridine (33.1), and this is the same relative order for the UV−vis bands of (Pc)AlCl and the molar absorptivity of these bands under the given experimental conditions.

Effect of Solvent on Reduction Processes. Three reversible to quasi-reversible one-electron reductions are observed between 0.00 and −2.00 V vs SCE in each of the four investigated solvents. Examples of the cyclic voltammograms in the four solvents are shown in Figure 2, and a summary of the half-wave potentials for the three major reductions in each solvent is given in Table 2. There are also two or three additional reduction peaks with smaller currents located at potentials negative of the first reduction process. These small cathodic peaks are labeled with an asterisk in Figure 2 and associated with side reactions of the neutral or electroreduced compounds.

To evaluate the effect of solvent on half-wave potentials, a correlation was attempted between $E_{1/2}$ for the three major reductions in each solvent and the Gutmann donor number (DN) of the solvent. Correlations between redox potentials and solvent properties such as donor number (DN), acceptor number (AN), or dielectric constant (ϵ) have proven in the past[26−30] to be quite useful not only for comparing the potentials of a given redox couple in a variety of different nonaqueous solvents but also for determining the nature of any interactions which might occur between the solvent and the oxidized or reduced forms of the compound. In the present study, the measured $E_{1/2}$ values for the first three reductions of (Pc)AlCl show no correlation with the solvent acceptor number, AN, or the solvent dielectric constant, ϵ.

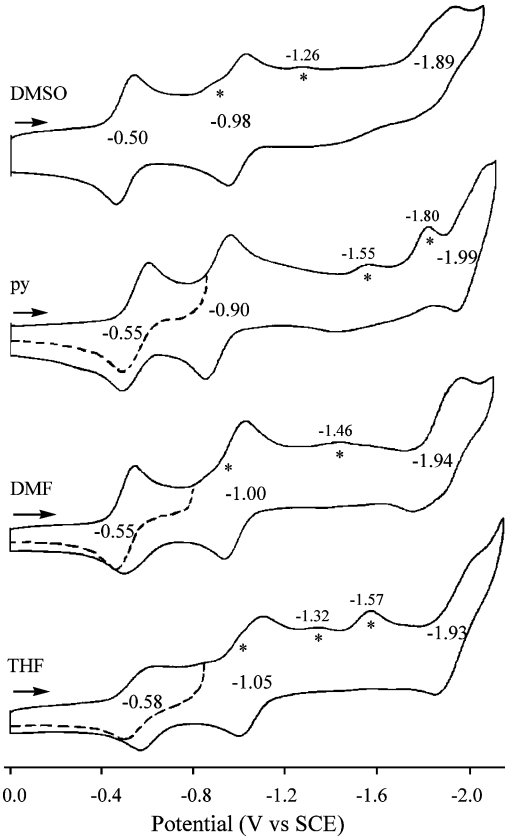

Figure 2. Cyclic voltammograms of (Pc)AlCl in different solvents containing 0.1 M TBAP as the supporting electrolyte (0.4 M TBAP for THF). Side reactions of the compounds are labeled with an asterisk. Scan rate = 0.1 V/s.

(25) Mack, J.; Stillman, M. In *The Porphyrin Handbook*; Kadish, K. M., Smith, K. M., Guilard, R., Eds.; Academic Press: Amsterdam, 2003; Vol. 16, Chapter 103, pp 43−116.
(26) Gutmann, V. *The Donor−Acceptor Approach to Molecular Interactions*; Plenum Press: New York, 1978.

Table 2. Half-wave Potentials (V vs SCE) in Different Solvents Containing 0.1 M TBAP[a]

		added anion[b]		$E_{1/2}$			
	solvent (DN)	type	concentration (equiv)	first	second	third	$E_{1/2}$ (Fc/Fc$^+$)
(Pc)AlCl	THF (20)[c]	none		−0.58	−1.05	−1.93	0.53
	DMF (26.6)	none		−0.55	−1.00	−1.94	0.52
	DMSO (29.8)	none		−0.50	−0.98	−1.89	0.50
	py (33.1)	none		−0.55	−0.90	−1.99	0.55
		Cl^-	33.0	−0.63	−0.90	−1.99	
	THF (20)[c]	Cl^-	8.0	−0.71	−1.05	−1.94	
		CN^-	35.1	−0.78	−1.04	−2.00[d]	
		OH^-	2.5	−0.94	−1.04	−1.93[d]	
		F^-	73.0	−0.95	−1.36	−1.94[d]	
(Pc)Al(OH)		none		−0.63	−1.02	e	
		OH^-	1.3	−0.99	−1.06	−1.92	

[a] Side reactions in Figure 2 are not listed. [b] Anion added in addition to TBAP as supporting electrolyte. [c] 0.4 M TBAP for THF. [d] E_{pc} at a scan rate of 0.1 V/s. [e] Ill-defined reduction because of μ-oxo dimer formation; see details in text.

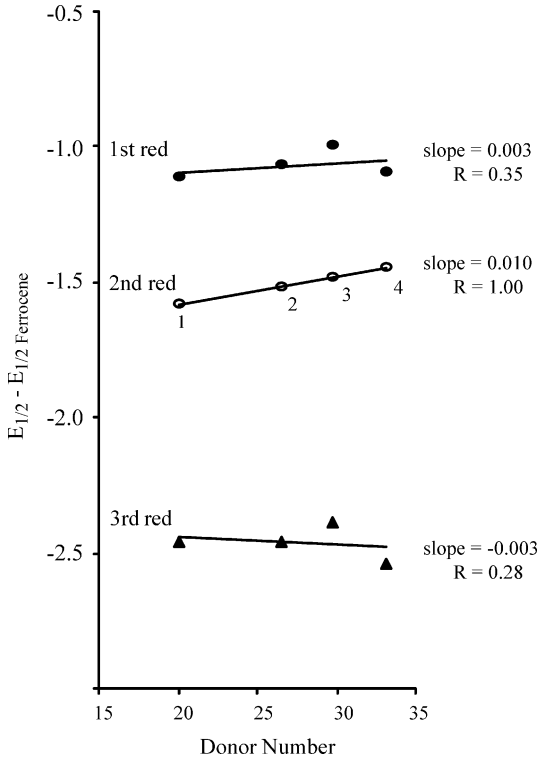

Figure 3. Plots of half-wave potentials (V vs Fc/Fc$^+$) for the three major reductions of (Pc)AlCl vs the Gutmann donor number of the solvent[26] (THF, DMF, DMSO, and py). Values of DN and $E_{1/2}$ for the compounds and the Fc/Fc$^+$ couple in each solvent are given in Table 2.

In contrast, a good linear relationship ($R = 1.00$) is obtained between DN and $E_{1/2}$ for the second reduction of the compound but not for the first or third reductions, as illustrated in Figure 3.

The initial reversible one-electron reduction of (Pc)AlCl in THF (DN = 20) is located at $E_{1/2} = -1.11$ V vs Fc/Fc$^+$, and an almost identical potential (−1.10 V vs Fc/Fc$^+$) is seen for reduction of this complex in pyridine (DN = 33.1). The invariance of $E_{1/2}$ between these two solvents indicates little or no solvent effect on the first reduction of the Al(III) phthalocyanine, and this is also seen in the plot of $E_{1/2}$ versus DN, where the slope is close to zero. This result indicates that, during the time scale of the electron transfer, solvent molecules are neither lost nor gained from the neutral compound upon conversion of (Pc)AlCl(S) to its singly reduced form (i.e., upon going from a Pc(2−) to a Pc(3−) macrocycle). In contrast, the positive linear relationship ($R = 1.00$) between $E_{1/2}$ for the second reduction and the DN of the solvent is consistent with the addition of a second solvent molecule to the doubly reduced complex (i.e., formation of $[(Pc)Al(S)_2]^-$ from (Pc)Al(S) in the Pc(3−)/Pc(4−) process). The most negative $E_{1/2}$ value for the second reduction (−1.58 V vs Fc/Fc$^+$) is seen in THF (DN = 20), while the most positive value (−1.45 V vs Fc/Fc$^+$) is observed in pyridine (DN = 33.1). The magnitude of the potential shift (130 mV) and its direction (positive) with increasing solvent donor number indicates a stronger stabilization of the doubly reduced species than the singly reduced form of the phthalocyanine on the time scale of the cyclic voltammetric experiment. This result might seen to contradict recent crystallographic data showing the formation of (•Pc)Al(THF)$_2$ after chemical reduction of (Pc)AlCl in THF,[19] but here, the experimental conditions are different. The product of the chemical reduction was isolated after 12 h of reflux in the presence of the reducing agent,[19] while at the electrode surface, the time to generate the Pc(3−) derivative is seconds rather than hours.

Finally, the third reduction of (Pc)AlCl occurs at −2.46 V vs Fc/Fc$^+$ in THF and −2.54 V vs Fc/Fc$^+$ in pyridine (Table 2), but the virtually zero slope of the $E_{1/2}$ versus DN plot (−0.003 V) and the R value of 0.28 (Figure 3) again indicate no meaningful correlation.

UV−Vis Monitoring of F^-, OH^-, or CN^- Binding to (Pc)AlCl(THF). The reactions of F^-, OH^-, and CN^- with (Pc)AlCl(THF) in THF were also monitored by electrochemistry and UV−vis spectroscopy during the stepwise addition of TBAX (X = F^-, OH^-, or CN^-) to a THF solution of the compound.

The spectroscopic changes monitored during the titration with TBAF·3H$_2$O are illustrated in Figure 4 and can be divided into three distinct regions of spectral transitions with

(27) Kelly, S. Y.; Kadish, K. M. *Inorg. Chem.* **1982**, *21*, 3631−3639.
(28) Bottomley, L. A.; Kadish, K. M. *Inorg. Chem.* **1981**, *20*, 1348−1357.
(29) Kadish, K. M.; Cornillon, J. L.; Yao, C. L.; Malinski, T.; Gritzner, G. *J. Electroanal. Chem.* **1987**, *235*, 189−207.
(30) Dubois, D.; Moninot, G.; Kutner, W.; Jones, M. T.; Kadish, K. M. *J. Phys. Chem.* **1992**, *96*, 7137−7145.

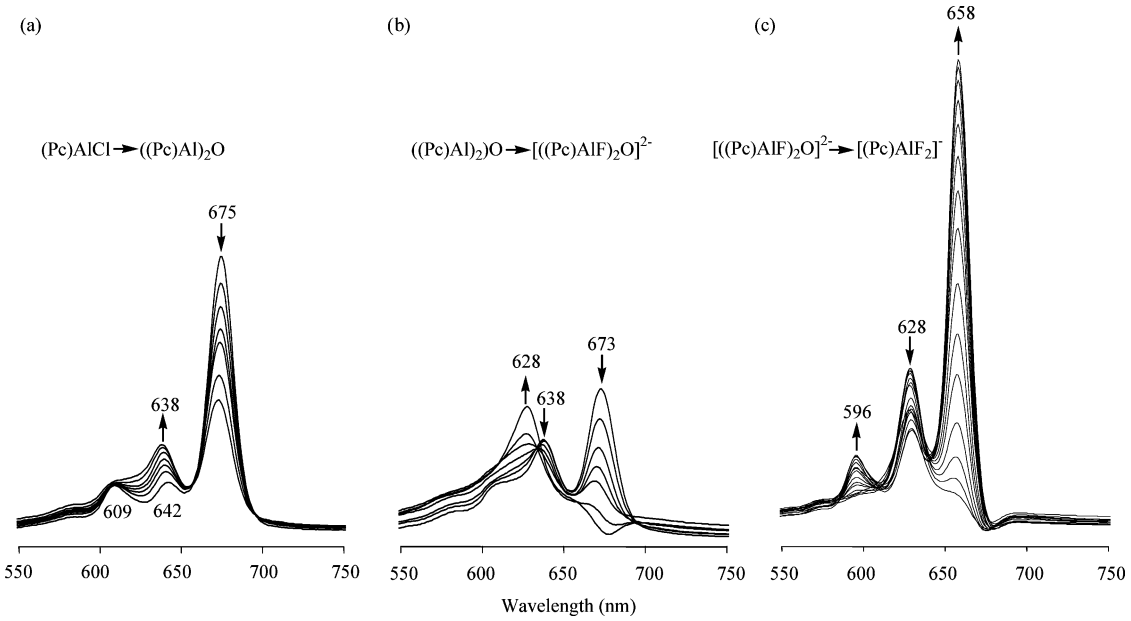

Figure 4. Spectroscopically monitored titration of 5.22×10^{-6} M (Pc)AlCl with TBAF·$3H_2O$ in THF: (a) first step (0−0.35 equiv of F^-), (b) second step (0.35−5.2 equiv of F^-), and (c) third step (5.2−86.4 equiv of F^-).

Scheme 1

$$(Pc^{2-})AlCl \xrightarrow[①]{TBAF\cdot 3H_2O} ((Pc^{2-})Al)_2O \xrightarrow[②]{F^-} [((Pc^{2-})AlF)_2O]^{2-} \xrightarrow[③]{F^-} [(Pc^{2-})AlF_2]^- \qquad (2)$$

675 638, 673 628 658, 632, 596 nm

$$(Pc^{2-})AlCl \xrightarrow[①]{OH^-} ((Pc^{2-})Al)_2O \xrightarrow[②]{OH^-} [((Pc^{2-})Al(OH))_2O]^{2-} \xrightarrow[③]{OH^-} [(Pc^{2-})Al(OH)_2]^- \qquad (3)$$

675 638, 675 665, 637, 602 nm

different sets of isosbestic points. Before addition of TBAF·$3H_2O$ to solution, the UV−vis spectrum has a major Q band at 675 nm and two weaker bands at 642 and 609 nm (see Table 1). In the first step of the titration (Figure 4a), the 675 nm band decreases by about 50% in intensity and shifts to 673 nm as a new Q band also grows in at 638 nm. The final UV−vis spectrum in Figure 4a was obtained after addition of 0.35 equiv of F^- (1.15 equiv of H_2O) in the form of TBAF·$3H_2O$ and is assigned to the μ-oxo dimer, $((Pc)Al)_2O$, on the basis of the two Q bands in the spectrum.

The spectral changes obtained upon the addition of 0.35−5.2 equiv of TBAF·$3H_2O$ to the same solution are shown in Figure 4b. Here, the bands at 673 and 638 nm disappear and are replaced by a single Q band at 628 nm. The final spectrum in Figure 4b is comparable with the spectrum reported for a bis-F^- μ-oxo dimer, $[((Pc)AlF)_2O]^{2-}$, which is characterized by $\lambda_{max} = 630$ nm.[17] The intensity of the 628 nm band decreases in intensity with further additions of TBAF·$3H_2O$, and the spectral changes obtained in solutions with 5.2−86.4 equiv F^- are shown in Figure 4c. The final spectrum in Figure 4c has a major Q band at 658 nm and two small bands at 632 and 596 nm. It is almost identical to the spectrum reported for the six-coordinate fluoride complex, $[(Pc)AlF_2]^{2-}$, which has a major Q band at 662 nm and two small bands at 633 and 596 nm.[17]

The overall spectral data in Figure 4 are consistent with the formation of transient five- and, then, six-coordinate μ-oxo dimers and with the sequence of steps shown in eq 2 (in Scheme 1) where the most intense Q band of each species are summarized in Table 3 and listed under the proposed form of the compound.

Table 3. Q Bands of Al(III) Phthalocyanines in THF

overall charge	species	λ_{max} (nm)			ref[a]
0	(Pc)AlCl	609	642	675	tw
	(Pc)AlOH	608	644	674	tw
	(Pc)Al(CN)	601	638	668	tw[b]
	$((Pc)Al)_2O$		638	673	tw[b]
−1	$[(Pc)Al(OH)_2]^-$	602	637	665	tw[b]
	$[(Pc)AlF_2]^-$	596	632	658	tw[b]
		596	633	662	17
−2	$[((Pc)AlF)_2O]^{2-}$		628		tw[b]
			630		17

[a] tw = this work. [b] In-situ-generated compounds (see text).

The above-described spectral changes and the formation of two transient μ-oxo dimers are also seen during the titration of (Pc)AlCl with TBAOH in THF where three regions of spectral transitions are again observed, as illustrated in Figure 5. At the start of the titration with OH^- (Figure 5a), the intensity of the 675 nm band assigned to (Pc)AlCl(THF) decreases, and a new band is observed at 638 nm. The final spectrum in the first step of the titration with OH^- is similar to the final spectrum in the first step of the titration with F^- (Figure 4a) and is assigned to $((Pc)Al)_2O$ in both cases. The 638 nm band of the μ-oxo dimer then shifts to 633 nm, and the 675 nm band further decreases in intensity as more

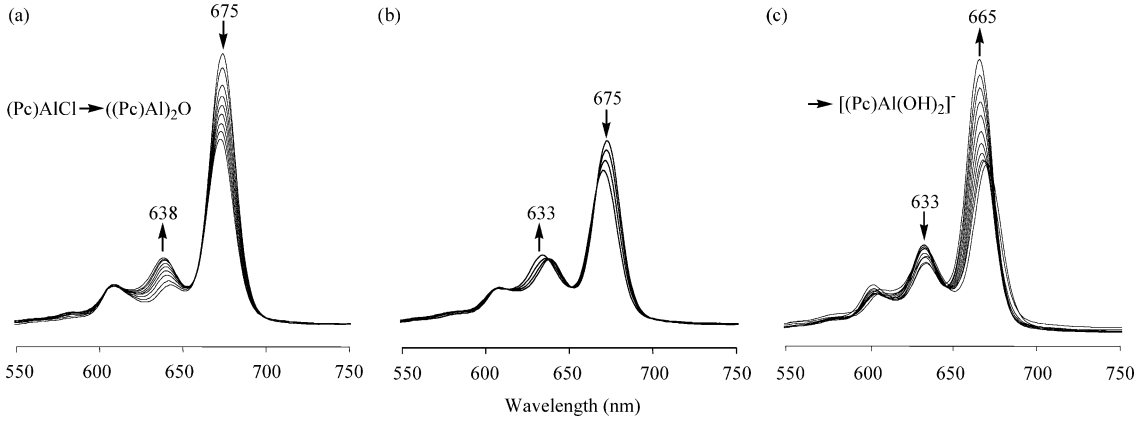

Figure 5. Spectroscopically monitored titration of 4.46×10^{-6} M (Pc)AlCl with TBAOH in THF: (a) first step (0−0.6 equiv of OH^-), (b) second step (0.6−1.1 equiv of OH^-), and (c) third step (1.1−25.6 equiv of OH^-).

TBAOH is added to solution during the second step of the titration (Figure 5b). Finally, in the third step of the titration, as more TBAOH is added to solution, a new intense band at 665 nm begins to form, and this band increases in intensity until it reaches a maximum after about 26 equiv of TBAOH have been added (Figure 5c). The final spectrum has bands at 665, 637, and 602 nm and is assigned to the monomeric Al(III) six-coordinate complex, $[(Pc)Al(OH)_2]^-$ on the basis of a similar spectrum for $[(Pc)AlF_2]^-$ (λ_{max} = 658, 632, and 596 nm).

On the basis of the data in Figure 5, the reaction sequence during the titration of (Pc)AlCl with TBAOH in THF is proposed to occur as shown in eq 3 (in Scheme 1) where two transient μ-oxo dimers are again observed in the conversion of (Pc)AlCl(THF) to $[(Pc)Al(OH)_2]^-$.

In contrast to what is spectrally observed during the F^- and OH^- titrations, quite different changes in the UV−vis spectra are obtained upon addition of TBACN to (Pc)AlCl-(THF) in THF. Under these solution conditions, the major Q band of (Pc)AlCl(THF) increases rather than decreases in intensity and shifts from 675 to 668 nm as CN^- is added to solution. At the same time, the two weaker bands of the starting compound in the visible region also increase in intensity and shift from 609 and 642 to 601 and 639 nm. The final UV−vis spectrum in the titration is assigned to (Pc)Al(CN)(THF). There is no spectral evidence for transient μ-oxo dimer formation during the CN^- titration nor is there any evidence for formation of a six coordinate CN^- complex at the end of the titration.

A summary of the Q band positions for the five in-situ-generated compounds in THF is given in Table 3 along with UV−vis data for genuine (Pc)AlCl and (Pc)Al(OH). As seen in this table, the position of the most intense Q band can be related to the overall charge of the compound. The four phthalocyanines with a single anion and a net zero charge have a strong Q band at 668−675 nm; those with two bound anionic ligands and a single negative charge on the compound have a more intense Q band located at 658−665 nm, and the bis-F^- μ-oxo dimer, with an overall charge of −2, has a single weaker Q band at 628−630 nm.

Effect of Chloride Binding on (Pc)AlCl Electrochemistry. Two of the solvents, THF and py, were selected to investigate the strength of Cl^- binding to the neutral and singly reduced forms of the phthalocyanine. THF is considered to be the weakest-binding solvent of those used in the present study, while pyridine is the strongest, as reflected by their Gutmann donor numbers of 20 and 33.1, respectively.

As can be seen in Table 2 and Figure 2, (Pc)AlCl undergoes three reversible reductions at $E_{1/2}$ = −0.58, −1.05, and −1.93 V vs SCE in THF containing 0.4 M TBAP. The first reduction shifts negatively when excess Cl^- is added to solution in the form of TBACl (see Figure 6a, where $E_{1/2}$ has shifted from −0.58 to −0.71 V in the presence of 8 equiv of Cl^-), while the second and third reductions of the compound show no shift in $E_{1/2}$ upon addition of Cl^- (Figure 6a and Table 2). A diagnostic plot of $E_{1/2}$ versus log [TBACl][31,32] is given in Figure 6b and shows a slope of −59 mV per 10-fold change in [Cl^-] for the first reduction and 0.0 mV for the second. These results are self-consistent and indicate that one and only one bound Cl^- is dissociated during the first reduction, thus leading to the proposed electron-transfer reaction given in eq 4 where S = THF.

$$(Pc^{2-})AlCl(S) + e + S \rightleftharpoons (^{\bullet}Pc^{3-})Al(S)_2 + Cl^- \qquad (4)$$

We have no evidence for or against the binding of two THF molecules to the electrogenerated ($^{\bullet}$Pc)Al radical, but we have made this assignment on the basis of data in the literature which shows formation of a stable bis-THF radical, $(Pc)Al(THF)_2$, after the chemical reduction of (Pc)AlCl in THF.[19] The tendency of ($^{\bullet}$Pc)Al to bind two anionic axial ligands is also shown in later sections of this manuscript.

An electrochemically monitored titration with TBACl was also carried out in pyridine at room temperature and gave results strongly resembling what is seen in THF (see Figure S1). These results again confirm that one and only one Cl^- anion is bound to the neutral compound and that neither the singly reduced nor the doubly reduced forms of the phthalocyanine contain an axially coordinated Cl^- on the time

(31) Kadish, K. M. In *Iron Porphyrins, Part Two*; Lever, A. B. P., Grey, H. B., Eds.; Addison-Wesley: London, 1983; pp 161−249.
(32) Crow, D. R. *Polarography of Metal Complexes*; Academic Press: London, 1969.

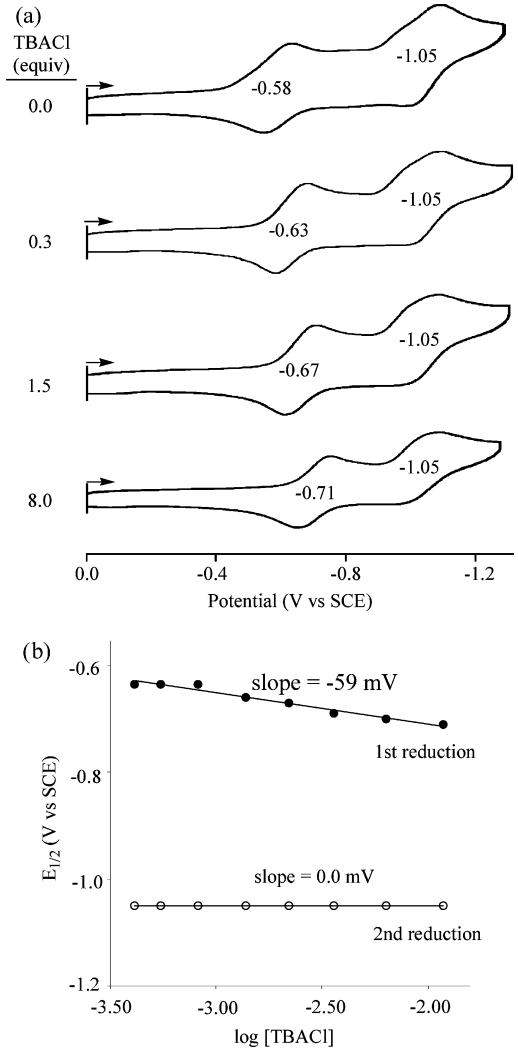

Figure 6. (a) Cyclic voltammograms showing the dependence of $E_{1/2}$ on added Cl^- for first two reductions of (Pc)AlCl in THF and (b) the relationship between $E_{1/2}$ and $[Cl^-]$. Scan rate = 0.1 V/s.

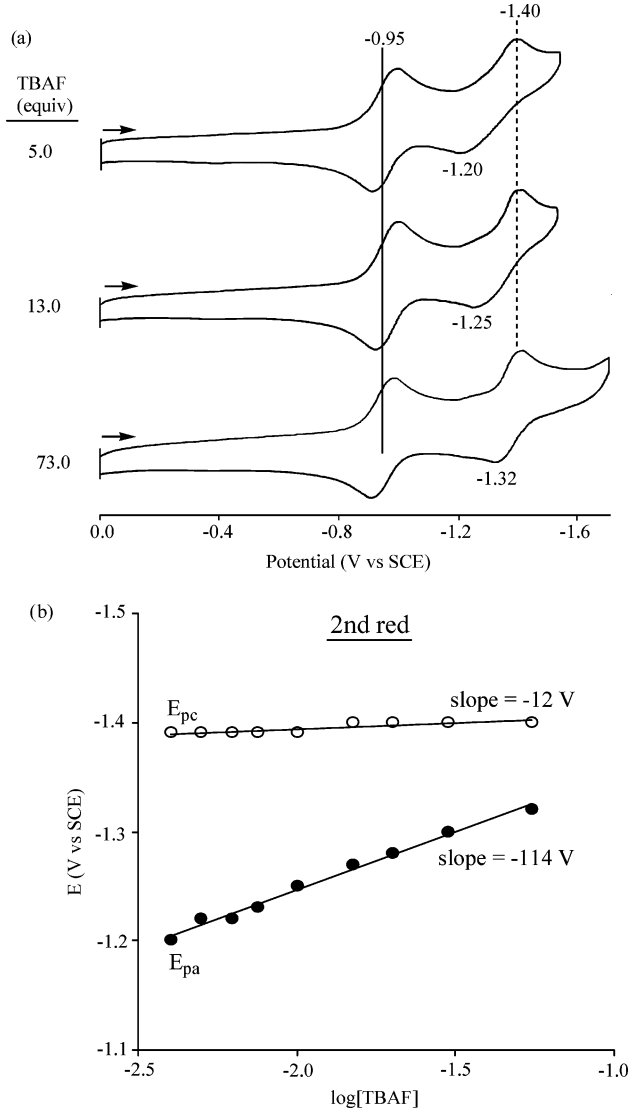

Figure 7. (a) Cyclic voltammograms showing the dependence of $E_{1/2}$ on added F^- for first two reductions of (Pc)AlCl in THF and (b) the relationship between the cathodic and anodic peak potentials and [TBAF]. Scan rate = 0.1 V/s.

scale of the electrochemical experiment. Under these conditions, the first reduction is described by eq 4 where S = py.

The fact that (Pc)AlCl(S) remains associated in both THF and py speaks for a strong binding of Cl^- to the Pc(3−) form of the phthalocyanine. Analysis of the data in Figures 6b and S1 and the use of appropriate equations given in the literature[31,32] leads to log K values of 4.2 and 3.2 for the ligand bindings of Cl^- as shown in eq 5 where X = Cl and S = THF and py, respectively.

$$[(Pc^{2-})Al(S)_2]^+ + X^- \rightleftharpoons (Pc^{2-})AlX(S) + S \qquad (5)$$

Electroreduction Mechanism in THF Containing Added F^-. The electroreduction mechanism of (Pc)AlCl(THF) in THF solutions containing F^- was evaluated by recording cyclic voltammograms as a function of increasing TBAF concentration and then constructing plots of half-wave or peak potential versus log [TBAF]. For the reversible Nernstian-controlled electron transfers, the slope of the $E_{1/2}$ versus log $[F^-]$ plot should be zero when no ligands are gained or lost during the electron transfer but will shift by 59/n mV per each 10-fold change of ligand concentration for each ligand added or lost during the process.[31,32] An example of this is shown in Figures 6b and S1 for the (Pc)AlCl reduction in THF or py solutions containing added TBACl.

Unfortunately, the second reduction of (Pc)AlCl in THF containing added F^- displays non-Nernstian behavior, and under these conditions, the analysis of the data involved plots being constructed with the individual anodic and cathodic peak potentials (E_{pa} and E_{pc}) rather than with the thermodynamic $E_{1/2}$ values. One such set of correlations is given in Figure 7, where the cathodic peak potentials for the first and second reductions of $[(Pc)AlF_2]^-$ both remain virtually constant from log [TBAF] = −3.0 to −1.8, while the second reoxidation peak potential shifts by −114 mV per 10 fold change of TBAF concentration. The spectroscopic data in Figure 4 indicates that $[(Pc)AlF_2]^-$ is the form of the phthalocyanine in solution prior to the electrochemistry being carried out, and thus, the constant E_{pc} values for the first and second reductions of $[(Pc)AlF_2]^-$ with an increase in added F^- (Figure 7a) can be uniquely accounted for by the

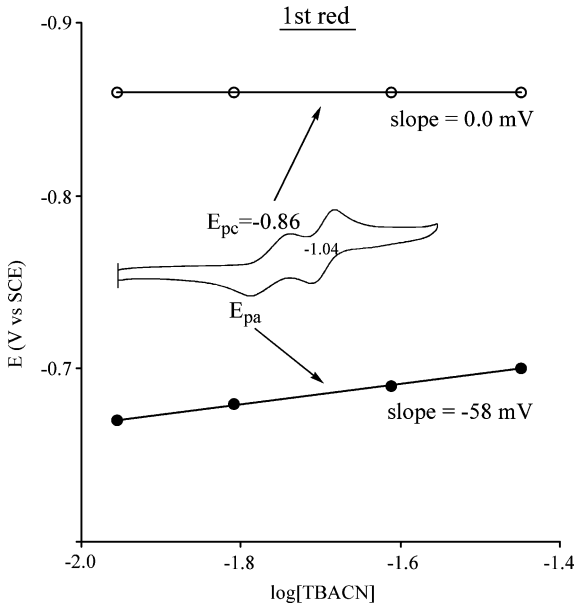

Figure 8. Relationship between cathodic and anodic peak potentials and added [CN^-] for the first reduction of (Pc)AlCl in THF. Scan rate = 0.1 V/s.

stepwise electron-transfer reactions given in eqs 6a and 6b.

$$[(Pc^{2-})AlF_2]^- + e \rightleftharpoons [(^{\bullet}Pc^{3-})AlF_2]^{2-} \quad E_{1/2} = -0.95\ V \tag{6a}$$

$$[(^{\bullet}Pc^{3-})AlF_2]^{2-} + e \rightleftharpoons [(Pc^{4-})AlF_2]^{3-} \quad E_{1/2} = -1.36\ V \tag{6b}$$

The reduction products of eqs 6a and 6b are stable on the cyclic voltammetry time scale, but on the longer time scale of spectroelectrochemistry, $[(Pc)AlF_2]^{3-}$ undergoes a slow loss of both axial ligands so that the overall reaction which actually occurs on the second reduction is that shown in eq 6c.

$$[(^{\bullet}Pc^{3-})AlF_2]^{2-} + e \overset{-1.36\ V}{\rightleftharpoons} [(Pc^{4-})AlF_2]^{3-} \overset{-2F^-}{\rightleftharpoons} [(Pc^{4-})Al]^- \tag{6c}$$

The doubly reduced $[(Pc)Al]^-$ formed at $E_{pc} = -1.40$ V can be reoxidized to give $[(^{\bullet}Pc)AlF_2]^{2-}$ on the reverse positive potential sweep, and this reformation of the bis-fluoride Pc(3−) species accounts for the −114 mV slope of the E_{pa} versus log [TBAF] plot describing the Pc(4−) to Pc(3−) oxidation reaction. A further reversible reoxidation of Pc(3−) to Pc(2−) then occurs without change in the number of axial ligands, and this second reoxidation proceeds as shown in eq 6a.

Electroreduction Mechanism in THF Containing Added CN^-. The above-described spectroscopic monitoring of TBACN addition to THF solutions of (Pc)AlCl(THF) shows formation of (Pc)Al(CN)(THF) in solution, and the electrochemistry of this in-situ-generated species, here represented as (Pc)Al(CN), was monitored in THF containing increasing concentrations of added CN^-. An analysis of the peak potentials for the first reduction and reoxidation of (Pc)Al(CN) is shown in Figure 8. The first reduction in THF containing greater than 10^{-2} M CN^- occurs at a constant $E_{pc} = -0.86$ V for a scan rate of 0.1 V/s indicating the

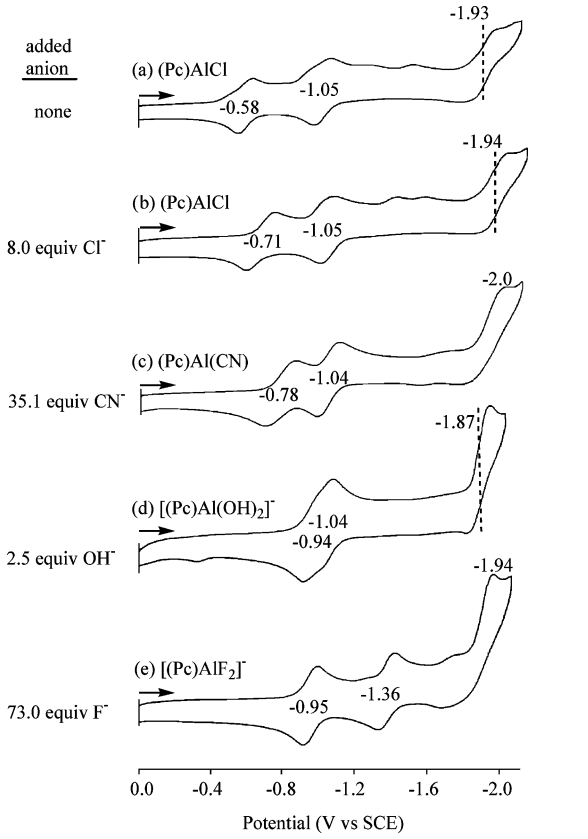

Figure 9. Cyclic voltammograms of (Pc)AlCl in THF containing 0.4 M TBAP and added anions in the form of TBAX where X = Cl^-, CN^-, OH^-, or F^-. The species labeled in parts c−e are in situ generated (see text for details). Scan rate = 0.1 V/s.

conversion of (Pc)Al(CN) to $[(^{\bullet}Pc)Al(CN)]^-$ without loss of the CN^- ligand on the time scale of the electron transfer. However, the CN^- from electrogenerated $[(^{\bullet}Pc)Al(CN)]^-$ dissociates prior to the second reduction giving the neutral radical ($^{\bullet}Pc$)Al as indicated by the measured $E_{1/2} = -1.04$ V for this process, a potential exactly the same as that for the second reduction of the (Pc)AlCl or (Pc)Al(OH), both of which also lose their axial ligands after the first electron transfer.

The electrogenerated neutral ($^{\bullet}Pc$)Al radical can also be reoxidized to give (Pc)Al(CN) at potentials between −0.50 and −0.70 V, depending on the concentration of CN^- in solution. This latter process occurs as shown in eq 7 and results in a −58 mV shift in plots of E_{pa} versus log [TBACN] (Figure 8).

$$(^{\bullet}Pc^{3-})Al \overset{-e + CN^-}{\rightleftharpoons} (Pc^{2-})Al(CN) \tag{7}$$

Although not strictly correct from a theoretical point of view, a quite reliable equilibrium constant for CN^- binding to $[(Pc)Al(THF)_2]^+$ can be calculated from the Nernstian slope of −58 mV in the E_{pa} versus log [TBACN] plot shown in Figure 8. The calculated log K value was 4.9 for the ligand binding reaction which is given by eq 3, where X = CN. The log K value of 4.9 is slightly larger than the log K value of 4.2 for Cl^- binding by $[(Pc)Al(THF)_2]^+$, and this is consistent with both the stronger coordinating ability of CN^- than that of Cl^- and the more negative reduction potential

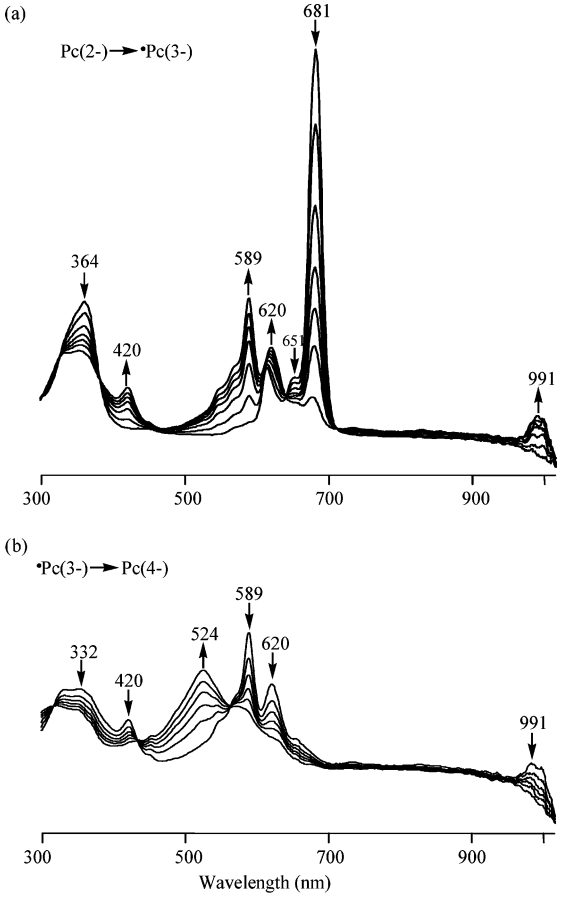

Figure 10. UV−vis spectral changes during the first two controlled potential reductions of (Pc)AlCl in pyridine containing 0.1 M TBAP: (a) $E_{app} = -0.60$ and (b) −1.00 V.

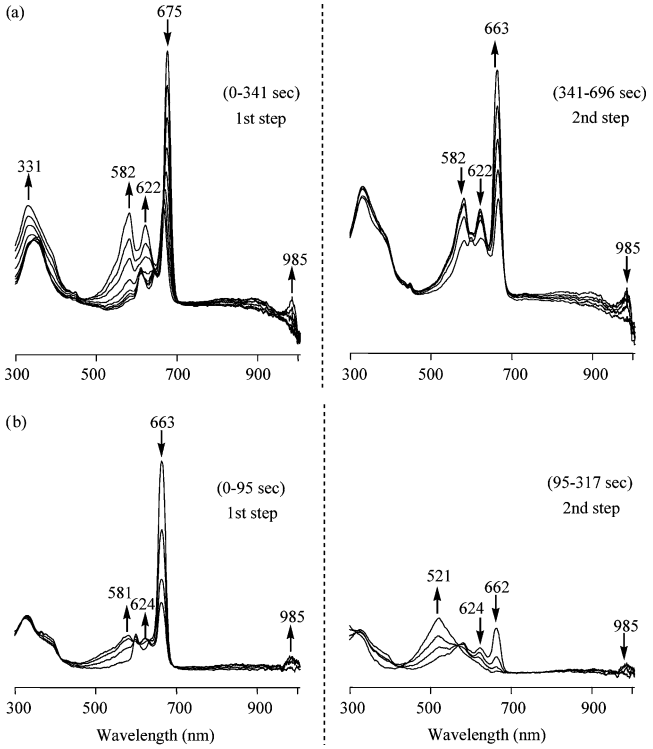

Figure 11. UV−vis spectral changes during the first two controlled potential reductions of (Pc)AlCl in THF containing 0.4 M TBAP. The final species generated after reduction at −0.80 V is assigned as $[(Pc)Al(OH)_2]^-$. (a) Initial reduction of (Pc)AlCl at −0.80 V in THF and (b) the reduction of the generated $[(Pc)Al(OH)_2]^-$ at −1.40 V.

for the Pc(2−)/Pc(3−) process of (Pc)Al(CN) in THF as compared to that in (Pc)AlCl (see Table 2).

Comparative Electrochemistry of (Pc)AlX and $[(Pc)AlX_2]^-$. The UV−vis data discussed above indicates formation of (Pc)Al(CN), $[(Pc)AlF_2]^-$, and $[(Pc)Al(OH)_2]^-$ in THF containing excess anions. Cyclic voltammograms of these three in-situ-generated compounds are shown in Figure 9c−e, along with voltammograms of (Pc)AlCl in THF with and without added Cl^-. The electrochemically examined $[(Pc)Al(OH)_2]^-$ was in situ generated in THF from (Pc)AlCl or (Pc)Al(OH) by the addition of TBAOH to solution (Figure S2), and it undergoes two reversible one-electron reductions at $E_{1/2} = -0.94$ and −1.04 V, as shown in Figure 9d. A third reduction of $[(Pc)Al(OH)_2]^-$ occurs at $E_{1/2} = -1.87$ V. The mono-hydroxo derivative, (Pc)Al(OH), is reversibly reduced at $E_{1/2} = -0.63$ and −1.02 V in THF (Figure S2) and thus has electrochemical behavior quite similar to that of (Pc)AlCl in this solvent.

The most obvious differences between the electrochemistry of the (Pc)AlX and $[(Pc)AlX_2]^-$ are the $E_{1/2}$ values for the first and second electroreductions, and on this basis of the cyclic voltammograms, they can be divided into two groups of compounds. The first comprises (Pc)Al(OH), (Pc)AlCl, and (Pc)Al(CN), which are uncharged and have an initial reduction potential between $E_{1/2} = -0.58$ and −0.78 V, depending upon the specific counteranion (OH^-, Cl^-, or CN^-) and the concentration added to solution in the form of TBAX. These compounds also undergo further reduction at virtually the same $E_{1/2}$ values of −1.04 to −1.05 V in THF (see Table 2).

The second group of compounds is represented by $[(Pc)Al(OH)_2]^-$ and $[(Pc)AlF_2]^-$. Both phthalocyanines are anionic, have similar UV−vis spectra (see Table 3), and are initially reduced at $E_{1/2} = -0.94$ or −0.95 V. A similar $E_{1/2} = -0.95$ V vs Ag/AgCl was reported for reduction of $[(Pc)AlF_2]^-$ in CH_2Cl_2,[17] and the negative shift in the reduction potential, as compared to the more easily reducible (Pc)AlX complexes, is consistent with the additional negative charge on the electroactive bis-F^- species which leads to a larger stabilization of the Pc(2−) form of the phthalocyanine than that of its singly reduced Pc(3−) form.

A second reduction potential was not previously reported in the literature for $[(Pc)AlF_2]^-$, and thus, a comparison between $E_{1/2}$ for this process in the present study and $E_{1/2}$ for the second reduction of $[(Pc)Al(OH)_2]^-$ can shed light on differences between these two compounds in their singly reduced form (i.e., Pc(3−)).

The second reduction of $[(Pc)Al(OH)_2]^-$ occurs at $E_{1/2} = -1.04$ V, a potential identical within the experimental error to the $E_{1/2}$ value for the reduction of the three zero-charged complexes, (Pc)Al(OH), (Pc)AlCl, and (Pc)Al(CN) (see Figure 9 and Table 2), which indicates that all anionic axial ligands have dissociated from the Al(III) center prior to the second reduction. In contrast, $E_{1/2}$ value is more negative at −1.36 V for the second reduction of $[(Pc)AlF_2]^-$. This fact,

Scheme 2

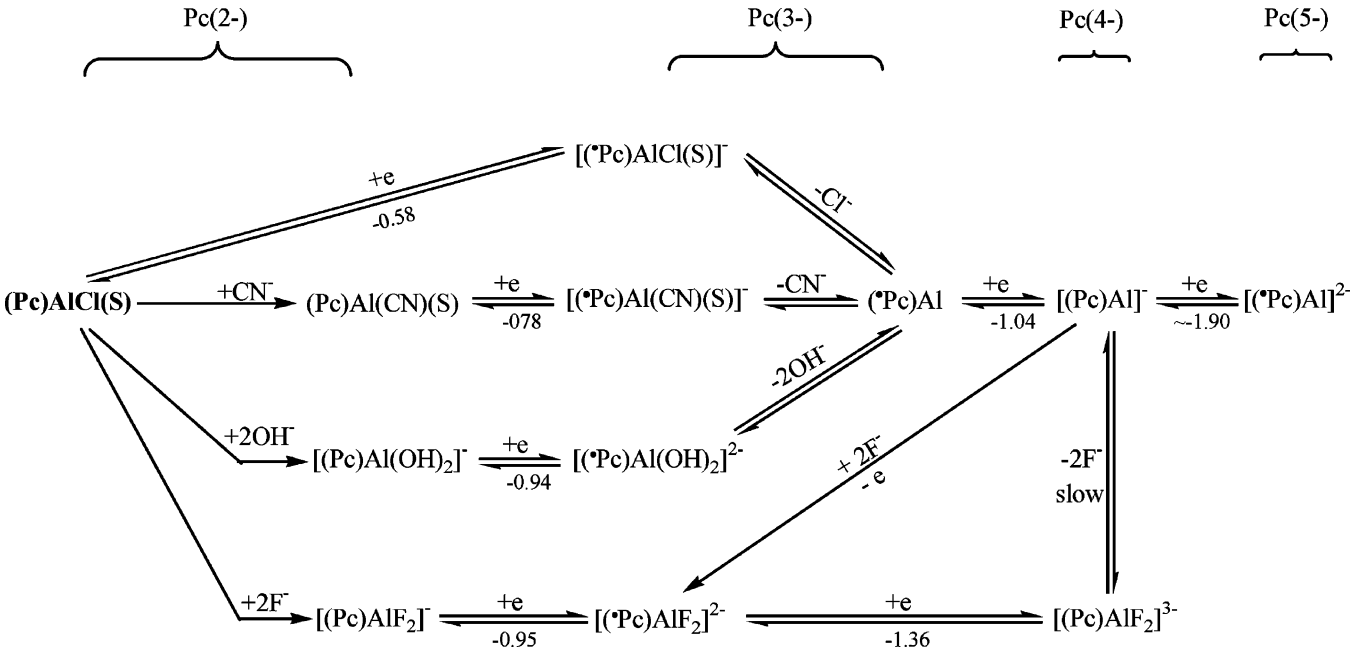

combined with the constant E_{pc} in solutions containing added TBAF (Figure 7), indicates that both the axially bound F^- ions remain bound to the metal center, at least on the electrochemical time scale of the first two one-electron additions. This being the case, the electroreduction mechanisms are different for the bis-OH^- and bis-F^- bound species, as compared to each other and also as compared to (Pc)AlCl in THF with added Cl^-, CN^-, OH^-, or F^-.

Finally, the third one-electron reduction of the five electrochemically examined compounds in THF occurs at a similar $E_{1/2}$ value of about −1.90 V (see Figures 9 and S2), independent of the initial charge on the compound or the type and number of anionic axial ligands bound to the initial Al(III) species. This clearly indicates that the doubly electroreduced product is the same in each case and is assigned as $[(Pc)Al]^-$.

These above-described electrode reactions are shown in Scheme 2 which illustrates the electroreduction mechanisms for each (Pc)AlCl(THF) complex in THF containing the different anions.

Spectroelectrochemistry in Pyridine. The one- and two-electron reduction products electrogenerated from (Pc)AlCl in py and in THF were both spectroscopically characterized in a thin-layer cell. The spectroelectrochemical data in pyridine is shown in Figure 10 where the first reduction was initially carried out at a controlled potential of −0.60 V, followed by further addition of a second electron when the applied potential was switched to −1.00 V.

The first reduction product in py has a well-defined Soret band at 420 nm and visible bands at 589, 620, and 991 nm (Figure 10a). A similar UV−vis spectrum was reported after reduction of the same compound in DMF[33] (λ_{max} = 575, 618, and 974 nm) and was assigned to the singly reduced neutral radical generated as shown in eq 2.

(33) Clack, D. W.; Yandle, J. R. *Inorg. Chem.* **1972**, *11*, 1738−1742.

The UV−vis spectral changes obtained during the second controlled potential reduction of (Pc)AlCl(py) to give the Pc(4−) complex in py are shown in Figure 10b. As the reduction proceeds, the intensity of the Pc(3−) bands at 420, 589, 620, and 991 nm decrease, and a new band assigned to Pc(4−) at 524 nm appears. The final spectrum in Figure 10b has major bands at 320 and 524 nm and can be compared with a similar spectrum in the literature (λ_{max} = 327 and 518 nm)[33] for the doubly reduced Al(III) complex in DMF. The Pc(3−)/Pc(4−) and Pc(3−)/Pc(2−) reactions are spectrally reversible, and the values of λ_{max} and ϵ for the Pc(3−) and Pc(4−) complexes in the different solvents are listed in Table 1.

Spectroelectrochemistry in THF. The spectral changes obtained during controlled potential reduction of (Pc)AlCl(THF) in THF (Figure 11) are more complicated than those in pyridine because of the presence of one or more coupled chemical reactions in the THF solvent. The spectral data obtained during each step in the reduction are summarized in Table 1, and a proposed mechanism for the overall reduction of (Pc)AlCl(THF) in THF on the spectroelectrochemical time scale is given in Scheme 3.

As the initial reduction proceeds at an applied potential of −0.80 V (reaction 1a), the band at 675 nm for the starting compound decreases in intensity, while three new bands of the singly reduced species appear at 582, 622, and 985 nm. This is shown in Figure 11a where the spectra were recorded from 0 to 341 s after the application of an applied potential. The final UV−vis spectrum obtained after 341 s is assigned as the neutral radical, $(•Pc^{3-})Al^{III}$, and is comparable with the spectrum of the one-electron reduction product in py (Figure 10a).

The electrogenerated Pc(3−) complex is unstable in THF and undergoes a slow homogeneous chemical reaction (reaction 1b) to give the spectral changes illustrated in

Scheme 3

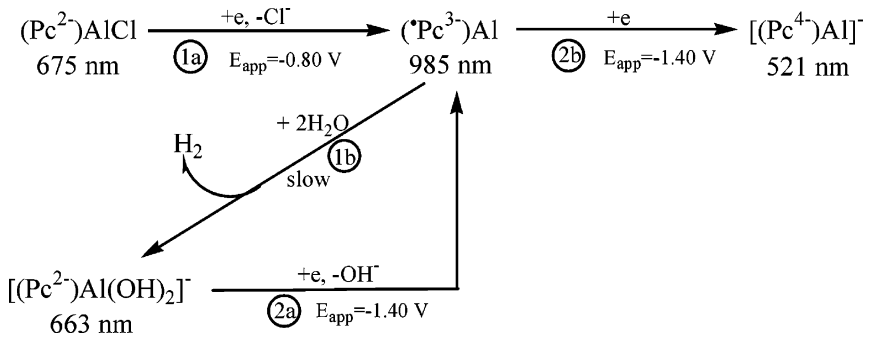

Figure 11b. As seen in this figure, an intense Q band appears at 663 nm and grows in intensity from 341 to 696 s after the start of electrolysis. The overall shape of the final spectrum resembles that of $[(Pc)Al(OH)_2]^-$ which can be generated by addition of TBAOH to (Pc)AlCl in THF (eq 4). Under the spectroelectrochemical conditions, the electrogenerated ($^{\bullet}Pc^{3-}$)Al(III) reacts with trace H_2O in the solvent (<0.005%) to give H_2 and $[(Pc)Al(OH)_2]^-$, the latter of which is spectroscopically observed.

The final UV−vis spectrum in Figure 11a does not revert to the spectrum of the initial species upon switching the potential back to 0.00 V, consistent with $[(Pc)Al(OH)_2]^-$ being stable in its Pc(2−) form at −0.80 V and not being reduced until more negative potentials because of the presence of the two axially bound OH^- ions. However, as expected, significant changes in the UV−vis spectra are observed after switching the applied potential from −0.80 to −1.40 V, where $[(Pc)Al(OH)_2]^-$ is reduced in two one-electron-transfer steps (Figure 9d). The first involves the conversion of Pc(2−) to Pc(3−) at $E_{1/2} = -0.94$ V (reaction 2a), and the second, at longer times, involves the conversion of Pc(3−) to Pc(4−) at $E_{1/2} = -1.04$ V (reaction 2b). The final UV−vis spectrum in Figure 11b after 317 s of applied potential is assigned as $[(Pc^{4-})Al]^-$. It has bands at 325 and 521 nm and is similar to the Pc(4−) form of the compound in py (Figure 10b), which is characterized by bands at 320 and 524 nm.

In summary, the thin-layer spectroelectrochemical reduction of (Pc)AlCl initially involves one electron to give the Pc(3−) complex, but this is followed by reformation of a Pc(2−) species assigned to $[(Pc)Al(OH)_2]^-$. There is no spectral evidence for formation of (Pc)Al(OH), $((Pc)Al)_2O$, or $[((Pc)Al(OH))_2O]^{2-}$ during the initial thin-layer electroreduction of (Pc)AlCl in THF nor is there any evidence for formation of these species during the electrochemical reduction of $[(Pc^{2-})Al(OH)_2]^-$ to give ($^{\bullet}Pc^{3-}$)Al. The μ-oxo and hydroxo species are also not observed in cyclic voltammograms of (Pc)AlCl to which OH^- has been added in the form of TBAOH (Figures 9d and S2).

Acknowledgment. The support of the Robert A. Welch Foundation (K.M.K., Grant E-680) and the Jiangsu University Foundation (05JDG051) are gratefully acknowledged.

Supporting Information Available: Dependence of $E_{1/2}$ for the first two reductions of (Pc)AlCl in py containing increasing amounts of Cl^- (Figure S1) and cyclic voltammograms of (a) (Pc)AlCl and (b) (Pc)AlOH in THF, before and after the addition of OH^-, 0.4 M TBAP (Figure S2). This material is available free of charge via the Internet at http://pubs.acs.org.

IC061072F